

# LENSING EFFECT ON THE RELATIVE ORIENTATION BETWEEN THE COSMIC MICROWAVE BACKGROUND ELLIPTICITIES AND THE DISTANT GALAXIES

L. VAN WAERBEKE<sup>1</sup>, F. BERNARDEAU<sup>2</sup>, K. BENABED<sup>2</sup>

*Draft version April 17, 2018*

## ABSTRACT

The low redshift structures of the Universe act as lenses in a similar way on the Cosmic Microwave Background light and on the distant galaxies (say at redshift about unity). As a consequence, the CMB temperature distortions are expected to be statistically correlated with the galaxy shear, exhibiting a non-uniform distribution of the relative angle between the CMB and the galactic ellipticities. Investigating this effect we find that its amplitude is as high as a 10% excess of alignment between CMB and the galactic ellipticities relative to the uniform distribution. The relatively high signal-to-noise ratio we found should make possible a detection with the planned CMB data sets, provided that a galaxy survey follow up can be done on a sufficiently large area. It would provide a complementary bias-independent constraint on the cosmological parameters.

*Subject headings:* cosmology: cosmic microwave background — cosmology: gravitational lensing — cosmology: large-scale structure of universe

## 1. INTRODUCTION

The analysis of gravitational lensing of the primordial fluctuations in the Cosmic Microwave Background (CMB) is of growing interest since it gives a direct probe of the mass distribution up to very high redshift. The detection of the lens effects on the CMB would be very precious for constraining the cosmological parameters, with no ambiguities about the distance of the source plane. Although the effect on the CMB power spectrum is rather weak and affects only small scales ( $l > 1000$ ) it is now recognized that gravitational lensing can produce some specific features worth for investigation. In this paper we focus our investigations on the temperature maps only although it has been noticed recently that lenses can also affect significantly the polarization properties of the CMB maps (Zaldarriaga & Seljak 1998a, Benabed & Bernardeau 1999).

So far there are two distinct effects that kept the attention: the small (sub-arcmin) scale strong deformation of the temperature fluctuations which can be used to probe galaxy cluster gravitational potential (Zaldarriaga & Seljak 1998b, Metcalf & Silk 1998) and an intermediate and large scale statistical effect (Bernardeau 1997, 1998, Seljak & Zaldarriaga 1999) which is a way to determine the cosmological parameters and provides a consistency test against other CMB analysis. The detection of the small scale lens effects, remains to be proved feasible. In particular the accumulation of secondary anisotropies (such as the Sunyaev-Zeldovich and Ostriker-Vishniac effects, and the non-linear Sachs-Wolfe effect) will mask the primordial lens effects and make the interpretation of lensed secondary anisotropies dependent on the *unknown* redshift where the secondary anisotropies were generated. At scales above 1 or 2 arcmins, the interpretation of the lens effects should be more straightforward but the number density of fluctuations is not large enough to allow an accurate mass reconstruction of the lens (in particular in the case of clusters of galaxies). Therefore at scales larger

than a few arcmin only a statistical detection of the lens effect seems possible. More specifically Bernardeau (1998) investigated the effect of lensing by the large-scale structures on the distribution of the CMB ellipticities. The consequences are the same as for the lensed distant galaxies: the gravitational distortion induces an excess of elongated structures of CMB ellipticities. The intrinsic CMB ellipticity distribution being known for a Gaussian field (e.g. Bond & Efstathiou 1987) it is then possible to compute the lensed distribution. The lensed distribution is unfortunately rather close to the unlensed one, in particular because the smoothing caused by the CMB beam tends to circularize the local structures. The orientation of the local ellipticity is expected to be much more robust against the smoothing effects and therefore more efficient in tracing the lens effects. Due to the low number density of structures on CMB maps such effects can be hardly detected in CMB maps alone, so in this paper we rather investigate the possible cross-correlation of CMB ellipticities with the distant galaxy ellipticities.

It has been recognized before that a fair fraction of the lenses that act on CMB temperature maps are at low redshift (Suginohara, Suginohara & Spergel 1998). There are different consequences. Temperature maps and galactic density survey should exhibit some correlations (Suginohara, Suginohara & Spergel 1998), and it induces a non-zero three-point function (or equivalently a bispectrum) in the CMB maps (Goldberg & Spergel 1998, Spergel & Goldberg 1998). This is due to the coupling between lens effects and low redshift primary or secondary anisotropies such as the integrated Sachs-Wolfe effect or the Sunyaev-Zeldovich effect.

In this paper we focus our analysis in the expected correlation between the CMB ellipticities and those of distant galaxies. We indeed expect their relative angle to be not-uniformly distributed unlike what would happen if there were no lensing effects. We examine here the am-

<sup>1</sup>CITA, 60 St George Str., Toronto, M5S 3H8, Canada

<sup>2</sup>SPhT, C.E. de Saclay, F-91191 Gif-sur-Yvette Cedex, France

plitude and the observability of this effect. It is worth stressing that, unlike in the analysis performed by Sugino-hara, Sugino-hara & Spergel 1998, the correlation signal we are aiming at is independent on any possible galaxy bias. It would then provide a complementary constraint on the fundamental cosmological parameters a priori independent on those provided by the observations of the primary anisotropies.

We discuss the physical mechanism, and introduce the relevant quantities in Section 2. In Section 3 we investigate the amplitude of the effect for different cosmologies and we calculate the signal-to-noise ratio in Section 4. Section 5 is a discussion on the contribution of the different possible foreground contaminations before we conclude in Section 6.

## 2. LENSING OF CMB ELLIPTICITIES

A bundle of light rays coming from a high redshift source from the direction  $\boldsymbol{\theta} = (\theta_x, \theta_y)$  is deflected by a quantity  $\boldsymbol{\xi}(\boldsymbol{\theta})$ , whose derivatives  $\kappa = \nabla \cdot \boldsymbol{\xi}$  and  $\boldsymbol{\gamma} = (\partial_x \xi_x - \partial_y \xi_y, 2\partial_x \xi_y)$  describe the isotropic and anisotropic deformation of the light bundle. The convergence  $\kappa$  and the shear  $\boldsymbol{\gamma}$  depend on the integrated gravitational potential along the line-of-sight  $\boldsymbol{\theta}$  and distort the image of distant galaxies as well as the CMB fluctuations.

At any position on the CMB temperature map, we can define an ellipticity  $\mathbf{e}$  from the curvature of the temperature field  $\delta_T$ :

$$\mathbf{e} = \left( \frac{\partial_x^2 \delta_T - \partial_y^2 \delta_T}{\partial_x^2 \delta_T + \partial_y^2 \delta_T}; \frac{2\partial_{xy} \delta_T}{\partial_x^2 \delta_T + \partial_y^2 \delta_T} \right). \quad (1)$$

This relation is similar to the ellipticity of a galaxy defined from its second order moments. A peak of temperature with the same curvature on both axis has a zero ellipticity, but in opposition with the galaxies, the CMB ellipticity can take any value between zero (circular peaks) and infinity (symmetric saddle points). However, it is always meaningful to define the orientation of the CMB ellipticity  $\theta_e = \arctan(e_2/e_1)$ , which runs from 0 to  $2\pi$ . The gravitational lensing effect tends to stretch the structures and therefore to produce an excess of elongated structures relative to the number of rather round objects (Bernardeau (1998)). The lenses tend also to align the CMB ellipticity with the shear  $\boldsymbol{\gamma}(\boldsymbol{\theta})$  acting on the CMB at the angular position  $\boldsymbol{\theta}$ . This is similar to the effect which occurs on the ellipticity of distant galaxies, although the corresponding shear  $\boldsymbol{\gamma}_g(\boldsymbol{\theta})$  cannot be identified with  $\boldsymbol{\gamma}(\boldsymbol{\theta})$  since the galaxies are at much lower redshift. The variables  $\boldsymbol{\gamma}(\boldsymbol{\theta})$  and  $\boldsymbol{\gamma}_g(\boldsymbol{\theta})$  are however correlated because the light coming from either the CMB or the distant galaxies are passing through the same portion of low-redshift Universe, and consequently, for a given line-of-sight  $\boldsymbol{\theta}$ , the CMB ellipticities are preferentially aligned with the distant galaxies.

In the paradigm of inflation, the CMB fluctuations are Gaussian. Therefore the un-lensed CMB ellipticity distribution is very specific and furthermore independent on the shape of the temperature power spectrum (Bond & Efstathiou 1987). The effect of gravitational lensing on the statistic of a Gaussian random field can be calculated analytically, at least using perturbative methods. According to (1), the fields of interest are the second derivatives of the temperature field, which defines the CMB ellipticity.

It is useful to introduce the matrix of the second order derivatives  $\mathcal{C}$

$$\mathcal{C} = \begin{pmatrix} \partial_x^2 \delta_T & \partial_{xy} \delta_T \\ \partial_{xy} \delta_T & \partial_y^2 \delta_T \end{pmatrix} = \begin{pmatrix} \tau + g_1 & g_2 \\ g_2 & \tau - g_1 \end{pmatrix}, \quad (2)$$

where the CMB ellipticity (1) is defined as in Bond & Efstathiou (1987) as,

$$\mathbf{e} = \frac{\mathbf{g}}{2\tau}. \quad (3)$$

We want to calculate the effect of lensing on  $\mathbf{e}$  and write the lensed ellipticity  $\hat{\mathbf{e}}$  as a function of  $\mathbf{e}$ , the shear  $\boldsymbol{\gamma}$  and the convergence  $\kappa$ . For this we need to calculate the lensed quantities  $\hat{\mathbf{g}}$  and  $\hat{\tau}$  and expand the expressions using the weak lensing approximation  $(\boldsymbol{\gamma}, \kappa) \ll 1$ .

The effect of weak lensing is only a re-mapping of the temperature fluctuations through the displacement field  $\boldsymbol{\xi}(\boldsymbol{\theta})$ , with no modification of the temperature amplitude,

$$\delta_T^{\text{obs}}(\boldsymbol{\theta}) = \delta_T^{\text{prim}}(\boldsymbol{\theta} + \boldsymbol{\xi}(\boldsymbol{\theta})). \quad (4)$$

The magnification matrix is the Jacobian of the transformation between the source and the image plane. It is given by the first derivatives of the displacement field:

$$\mathcal{A}_{ij} = \delta_{ij}^K + \xi_{i,j} = \begin{pmatrix} 1 - \kappa - \gamma_1 & -\gamma_2 \\ -\gamma_2 & 1 - \kappa + \gamma_1 \end{pmatrix}, \quad (5)$$

where  $\kappa$  is the convergence and  $\boldsymbol{\gamma}$  the shear. The lensed curvature matrix calculated from Eq.(2) and (4) is (Bernardeau 1998):

$$\mathcal{C}_{ij}^{\text{obs}} = \mathcal{A}_{ik} \mathcal{C}_{kl}^{\text{prim}} \mathcal{A}_{lj} + (\partial_k \delta_T)(\partial_j \xi_{k,i}) \quad (6)$$

The first term is identical to the lensing term for galaxies, and the second term makes intervene the spatial derivatives of  $\kappa$  and  $\boldsymbol{\gamma}$ . This second term accounts for the variation of the amplification matrix across the CMB patterns. It cannot be a priori neglected because the scale at which the shear is estimated corresponds roughly to the filtering scale, a scale over which the shear might significantly change. Note that for the galaxy field, the shear is measured at a much smaller scale (the galaxy size), and the shear gradient term is always neglected. However we will assume later that the shear field is Gaussian (which is a reasonable approximation for scales larger than a few arcmin), for which the shear gradient is uncorrelated to the shear itself. Therefore we expect the shear gradients to play no role in the cross-correlation pattern. As a result, in the following, the second term of Eq. (6) will be ignored for the lensed CMB ellipticities as well.

It is then easy to obtain the transformation equations for  $\tau$  and  $\mathbf{g}$ :

$$\begin{aligned} \hat{\tau} &\simeq \tau(1 - 2\kappa) + 2\boldsymbol{\gamma} \cdot \mathbf{g} \\ \hat{\mathbf{g}} &\simeq \mathbf{g}(1 - 2\kappa) + 2\tau\boldsymbol{\gamma}. \end{aligned} \quad (7)$$

The lensed ellipticity  $\hat{\mathbf{e}}$  is obtained from Eq.(3) and (7):

$$\hat{\mathbf{e}} \simeq \mathbf{e} + 4(\boldsymbol{\gamma} \cdot \mathbf{e})\mathbf{e} - \boldsymbol{\gamma} \quad (8)$$

Note that this is very similar to the galaxy ellipticity transformation relations (Schneider & Seitz 1995) for which we have  $\hat{\boldsymbol{\epsilon}} \simeq \boldsymbol{\epsilon} - (\boldsymbol{\gamma} \cdot \boldsymbol{\epsilon})\boldsymbol{\epsilon} + \boldsymbol{\gamma}$  if  $\boldsymbol{\epsilon}$  is the intrinsic galaxy ellipticity. It is remarkable that the lensed ellipticity does not depend on the convergence  $\kappa$ .

### 3. GALAXY-CMB ELLIPTICITIES ORIENTATION

Let  $\theta$  be the angle between  $\hat{\mathbf{e}}$  and the shear  $\gamma(\boldsymbol{\theta})$  at the redshift of the CMB, and  $\theta_g$  the angle between  $\hat{\mathbf{e}}$  and the shear of the distant galaxies  $\gamma_g(\boldsymbol{\theta})$ :

$$\cos(\theta) = \frac{\hat{\mathbf{e}} \cdot \boldsymbol{\gamma}}{\hat{e}\gamma} ; \cos(\theta_g) = \frac{\hat{\mathbf{e}} \cdot \boldsymbol{\gamma}_g}{\hat{e}\gamma_g} \quad (9)$$

We should emphasize that the angles  $\theta, \theta_g$  are twice the physical angles measured from the temperature map and the distant galaxies (e.g.  $\theta_g = \pi$  means that a lensed temperature fluctuation is perpendicular to a sheared distant galaxy, if they were both intrinsically circular).

We want to calculate the probability distribution function  $\mathcal{P}(\theta_g)$  of the relative orientation between the lensed CMB ellipticity and the sheared distant galaxies. This can be done by marginalizing the joint probability  $\mathcal{P}(\hat{\mathbf{e}}, \gamma, \gamma_g, \theta, \theta_g)$  over  $(\hat{\mathbf{e}}, \gamma, \gamma_g, \theta)$ . We adopt the point of view of conditional probability and write  $\mathcal{P}(\hat{\mathbf{e}}, \gamma, \gamma_g, \theta, \theta_g)$  as,

$$\mathcal{P}(\hat{\mathbf{e}}, \gamma, \gamma_g, \theta, \theta_g) = \mathcal{P}(\hat{\mathbf{e}}|\boldsymbol{\gamma})\mathcal{P}_{\text{lens}}(\gamma, \gamma_g, \theta, \theta_g), \quad (10)$$

where  $\mathcal{P}_{\text{lens}}(\gamma, \gamma_g, \theta, \theta_g)$  (which is a pure lensing contribution), is the joint probability that the shear is  $\gamma$  at the last-scattering surface and  $\gamma_g$  for the distant galaxies.  $\mathcal{P}(\hat{\mathbf{e}}|\boldsymbol{\gamma})$  is the probability to observe a lensed CMB ellipticity  $\hat{\mathbf{e}}$  when the shear is  $\boldsymbol{\gamma}$  at the last-scattering surface. It is calculated from the ellipticity distribution function  $p(e)$  of the unlensed CMB (Bond & Efstathiou 1987):

$$p(e)de = p(e_1, e_2)ede = \frac{8e}{(1 + 8e^2)^{3/2}}de. \quad (11)$$

From the Eq.(8) and the weak lensing approximation ( $\gamma \ll 1$ ) we get,

$$\begin{aligned} P(\hat{\mathbf{e}}|\boldsymbol{\gamma}) &= P(\hat{e}_1, \hat{e}_2|\boldsymbol{\gamma})\hat{\mathbf{e}} = p(e_1, e_2) \left| \frac{\partial e_i}{\partial \hat{e}_j} \right| \hat{\mathbf{e}} \\ &\simeq \frac{8\hat{e}}{(1 + 8\hat{e}^2)^{3/2}} \left( 1 - 36 \frac{\hat{\mathbf{e}} \cdot \boldsymbol{\gamma}}{(1 + 8\hat{e}^2)} \right) \end{aligned} \quad (12)$$

The integration over  $\hat{\mathbf{e}}$  gives the desired probability (10) as a function of  $\mathcal{P}_{\text{lens}}$  only,

$$\mathcal{P}(\gamma, \gamma_g, \theta, \theta_g) = (1 - 3\sqrt{2}\gamma \cos(\theta))\mathcal{P}_{\text{lens}}(\gamma, \gamma_g, \theta, \theta_g). \quad (13)$$

At this stage we need a model for  $\mathcal{P}_{\text{lens}}(\gamma, \gamma_g, \theta, \theta_g)$ . Both the observables  $\hat{\mathbf{e}}$  and  $\boldsymbol{\gamma}_g$  will respectively be measured on the temperature fluctuation map and a galaxy survey. Due to the limited beam size of the bolometers, we cannot hope to measure  $\hat{\mathbf{e}}$  with a resolution better than a few arcmin. Let  $\theta_0^{\text{CMB}}$  be this beam size, and  $\theta_0$  be the smoothing length used to measure  $\gamma_g$ . These two smoothing scales can be totally different, and we will find later that the better signal-to-noise is obtained when they are equal. This discussion is left aside for now, and we assume in the following that  $\theta_0^{\text{CMB}}$  and  $\theta_0$  are both larger than a few arcmin. It is therefore reasonable to assume a Gaussian distribution for the variable  $\mathbf{V} = [\gamma, \gamma_g]$ , and to write  $\mathcal{P}_{\text{lens}}(\gamma, \gamma_g, \theta, \theta_g)$  as a multivariate Gaussian distribution,

$$P_{\text{lens}}(\gamma, \gamma_g, \theta - \theta_g) = \frac{1}{2\pi(\text{Det}\mathbf{M})^{1/2}} \exp[-\mathbf{V}\mathbf{M}^{-1}\mathbf{V}], \quad (14)$$

whose correlation matrix  $\mathbf{M}$  is given by

$$\mathbf{M} = \begin{pmatrix} \langle \gamma^2 \rangle & \langle \gamma\gamma_g \rangle \\ \langle \gamma\gamma_g \rangle & \langle \gamma_g^2 \rangle \end{pmatrix} = \frac{1}{2} \begin{pmatrix} \sigma^2 & r\sigma\sigma_g \\ r\sigma\sigma_g & \sigma_g^2 \end{pmatrix}. \quad (15)$$

We used the property  $\langle \gamma_i\gamma_j \rangle = \delta_{ij}^K \langle \kappa^2 \rangle / 2$  (valid for the weak lensing limit), where  $\sigma^2 = \langle \kappa^2 \rangle$ ,  $\sigma_g^2 = \langle \kappa_g^2 \rangle$ .  $r = \langle \kappa\kappa_g \rangle / (\sigma\sigma_g)$  is the correlation coefficient of the shear amplitude between the CMB and the distant galaxies. Note that the probability (14) only depends on the relative orientation between  $\boldsymbol{\gamma}$  and  $\boldsymbol{\gamma}_g$  since we can choose any origin for the orientations. Figure 1 shows (for LCDM) the correlation function  $r$  for a fixed  $\theta_0^{\text{CMB}}$  as a function of  $\theta_0$ . The moments of the convergence are calculated using the perturbation theory and the non-linear evolution of the power spectrum given by Peacock & Dodds 1996. It is interesting to note on this figure that the maximum correlation is reached when  $\theta_0$  and  $\theta_0^{\text{CMB}}$  are nearly equal.

With a formal calculator Eq.(13) can be integrated without difficulties over  $\gamma, \gamma_g$  and  $\theta$  in order to get the final result:

$$\mathcal{P}(\theta_g)d\theta_g = \frac{d\theta_g}{2\pi} \left( 1 + 3\sqrt{\frac{\pi}{2}} \frac{\langle \kappa\kappa_g \rangle}{\langle \kappa^2 \rangle^{1/2}} \cos(\theta_g) \right). \quad (16)$$

This equation constitutes the main result of this paper. It shows how much the relative orientation of the CMB ellipticity with the distant galaxies deviates from a random distribution, because of the gravitational lensing effect.

Figure 2 shows the amplitude of this effect for different cosmological models and different smoothing scales. We assumed a CDM power spectrum taking into account its non-linear evolution as described by Peacock & Dodds 1996. The deviation from a uniform distribution can be as large as 10%, and the effect seems mostly sensitive to the curvature of the Universe rather than  $\Omega_M$  or  $\Lambda$ . A possible observable is the average of  $\cos(\theta_g)$  over the total survey area:

$$\langle \cos(\theta_g) \rangle = \frac{3}{2} \sqrt{\frac{\pi}{2}} \frac{\langle \kappa\kappa_g \rangle}{\langle \kappa^2 \rangle^{1/2}}. \quad (17)$$

If the CMB ellipticities are significantly aligned with the distant galaxies, then  $\langle \cos(\theta_g) \rangle$  should be significantly larger than zero. Some values of  $\langle \cos(\theta_g) \rangle$  are given in Table 1 for various cosmological models and smoothing schemes.

## 4. SIGNAL-TO-NOISE ANALYSIS

### 4.1. Description

In order to compute the signal-to-noise of the quantity (17), let us assume that we have at our disposal a CMB temperature map and a shear map of distant galaxies of angular area  $\mathcal{S}$ . An estimator  $E$  of  $\langle \cos(\theta_g) \rangle$  for a finite number  $N$  of measurements at locations  $\boldsymbol{\theta}_i$  is,

$$E = \frac{1}{N} \sum_{i=1}^N \cos[\theta_g(\boldsymbol{\theta}_i)]. \quad (18)$$

The ensemble average of the variance of this estimator is

$$\langle E^2 \rangle = \frac{\langle \cos^2(\theta_g) \rangle}{N} + \frac{N-1}{N} \int \frac{d^2\theta_1}{S} \int \frac{d^2\theta_2}{S} \times \langle \cos[\theta_g(\theta_1)] \cos[\theta_g(\theta_2)] \rangle. \quad (19)$$

The first term accounts for the variance due to the random intrinsic orientation of the ellipticities. The second term is the contribution of the cosmic variance.  $N$  can be either the number of individual galaxies or the number of cells in which the galaxy ellipticities are averaged. In any case, for  $S$  large enough it is reasonable to take  $N \rightarrow \infty$ <sup>3</sup>, for which only the cosmic variance term matters. Therefore the variance of  $\langle \cos(\theta_g) \rangle$  is approximated by

$$\sigma_{\langle \cos(\theta_g) \rangle}^2 \simeq \int_S \frac{d^2\theta_1}{S} \frac{d^2\theta_2}{S} \langle \cos[\theta_g(\theta_1)] \cos[\theta_g(\theta_2)] \rangle. \quad (20)$$

The correlator  $C = \langle \cos[\theta_g(\theta_1)] \cos[\theta_g(\theta_2)] \rangle$  depends on the temperature correlation function and on the convergence correlation function, and it has to be calculated from the joint probability  $\mathcal{P}(\gamma_g(\theta_1), \gamma_g(\theta_2), \hat{\mathbf{e}}(\theta_1), \hat{\mathbf{e}}(\theta_2))$ .

#### 4.2. Calculations

The calculations are simplified if we assume that the temperature fluctuations are un-lensed and uncorrelated with the orientation of the galaxies. This will give, by construction, the signal-to-noise of the CMB-lens positive detection against the hypothesis of no lensing on CMB. In that case the lensing and the CMB distribution functions are separable and can be written,

$$\mathcal{P}(\gamma_g(\theta_1), \gamma_g(\theta_2), \mathbf{e}(\theta_1), \mathbf{e}(\theta_2)) = \mathcal{P}_{\text{lens}}(\gamma_g(\theta_1), \gamma_g(\theta_2)) \mathcal{P}_{\text{CMB}}(\mathbf{e}(\theta_1), \mathbf{e}(\theta_2)). \quad (21)$$

Using Eq. (3), it is then possible to re-express the latter distribution in terms of the variables  $\mathbf{g}(\theta_1)$ ,  $\mathbf{g}(\theta_2)$ ,  $\tau_1$  and  $\tau_2$ , taking advantage of the fact that  $\mathcal{P}_{\text{CMB}}(\mathbf{g}(\theta_1), \mathbf{g}(\theta_2))$  follows a Gaussian distribution. Therefore  $\mathcal{P}_{\text{CMB}}(\mathbf{g}(\theta_1), \mathbf{g}(\theta_2))$  has the same form as in Eq.(14) with

$$\mathbf{V} = [\mathbf{g}(\theta_1), \mathbf{g}(\theta_2)] \\ \mathbf{M} = \frac{1}{2} \begin{pmatrix} \langle \tau^2 \rangle & \langle \tau(\theta_1)\tau(\theta_2) \rangle \\ \langle \tau(\theta_1)\tau(\theta_2) \rangle & \langle \tau^2 \rangle \end{pmatrix}, \quad (22)$$

here the correlation coefficient is defined as the temperature fluctuations taken at two different locations  $\theta_1$  and  $\theta_2$ . Similarly,  $\mathcal{P}_{\text{lens}}(\gamma_g(\theta_1), \gamma_g(\theta_2))$  is given by (14) with

$$\mathbf{V} = [\gamma_g(\theta_1), \gamma_g(\theta_2)] \\ \mathbf{M} = \frac{1}{2} \begin{pmatrix} \langle \kappa_g^2 \rangle & \langle \kappa_g(\theta_1)\kappa_g(\theta_2) \rangle \\ \langle \kappa_g(\theta_1)\kappa_g(\theta_2) \rangle & \langle \kappa_g^2 \rangle \end{pmatrix}. \quad (23)$$

We are now in position to calculate  $C$  in which we rewrite  $\cos[\theta_g(\theta_1)]$  (resp.  $\cos[\theta_g(\theta_2)]$ ) as  $\cos[\theta_{\mathbf{e}}(\theta_1) - \theta_{\text{gal}}(\theta_1)]$  (resp.  $\cos[\theta_{\mathbf{e}}(\theta_2) - \theta_{\text{gal}}(\theta_2)]$ ), where  $\theta_{\mathbf{e}}(\theta_1)$  is the orientation of the CMB ellipticity at location  $\theta_1$ , and  $\theta_{\text{gal}}(\theta_1)$  the

orientation of a galaxy at location  $\theta_1$ . It is useful to define  $\phi_{\mathbf{e}} = \theta_{\mathbf{e}}(\theta_1) - \theta_{\mathbf{e}}(\theta_2)$  and  $\phi_{\text{gal}} = \theta_{\text{gal}}(\theta_1) - \theta_{\text{gal}}(\theta_2)$ , and to express  $\mathcal{P}_{\text{lens}}(\gamma_g(\theta_1), \gamma_g(\theta_2))$  and  $\mathcal{P}_{\text{CMB}}(\mathbf{g}(\theta_1), \mathbf{g}(\theta_2))$  as a function of  $\cos(\phi_{\text{gal}})$  and  $\cos(\phi_{\mathbf{e}})$  respectively. Then the only non-vanishing term in the correlator  $C$  is

$$C = \frac{1}{2} \langle \cos(\phi_{\mathbf{e}}) \cos(\phi_{\text{gal}}) \rangle. \quad (24)$$

The calculation of  $C$  makes intervene the normalized correlation functions  $c_{\kappa} = \langle \kappa(\theta_1)\kappa(\theta_2) \rangle / \langle \kappa^2 \rangle$  and  $c_{\tau} = \langle \tau(\theta_1)\tau(\theta_2) \rangle / \langle \tau^2 \rangle$ . It turns out that the calculation of (24) is tractable analytically if we assume that  $c_{\kappa}$  and  $c_{\tau}$  are small compared to unity (then we can expand the distribution function with respect to  $c_{\kappa}$  and  $c_{\tau}$ ). This is always a well justified approximation for large surveys as those discussed here (for which the  $c$  coefficients are at percent level). After a straightforward manipulations (that can easily be done with a formal calculator) we find

$$\langle \cos[\theta_g(\theta_1)] \cos[\theta_g(\theta_2)] \rangle \simeq \frac{1}{2} \left( \frac{c_{\tau}^2}{2} + \frac{7c_{\tau}^4}{48} + \dots \right) \frac{\pi}{32} (8c_{\kappa} + c_{\kappa}^3 + \dots). \quad (25)$$

The leading order in the correlation coefficient  $c_{\tau}$  and  $c_{\kappa}$  is thus:

$$\langle \cos[\theta_g(\theta_1)] \cos[\theta_g(\theta_2)] \rangle = \frac{\pi}{16} \left[ \frac{\langle \tau(\theta_1)\tau(\theta_2) \rangle}{\langle \tau^2 \rangle} \right]^2 \frac{\langle \kappa(\theta_1)\kappa(\theta_2) \rangle}{\langle \kappa^2 \rangle}, \quad (26)$$

which has to be integrated over the survey size in order to give the desired result (20).

#### 4.3. Temperature and convergence correlation functions

In order to estimate (26) one needs the temperature and the convergence correlation functions.

The temperature correlation function can be evaluated from the angular CMB power spectrum  $C_l$  given by the CMBFAST code (Seljak & Zaldarriaga 1996). However, we have to include the beam size effect (which tends to enlarge the temperature correlation function and therefore to increase the noise) and to correct for the instrumental noise. This can be achieved by a suitable Wiener filtering of the power spectrum. The filtered  $\tilde{C}_l$  are given by

$$\tilde{C}_l = \frac{C_l e^{-l^2 \sigma_b^2}}{C_l e^{-l^2 \sigma_b^2} + C_{\text{noise}}} C_l e^{-l^2 \sigma_b^2}, \quad (27)$$

where  $\sigma_b = \theta_0^{CMB} / \sqrt{8 \log(2)}$  gives the beam size and  $C_{\text{noise}} = \sigma_{\text{pix}}^2 \Omega_{\text{pix}} \simeq 2.10^{-17}$  is the typical level of noise for experiments like MAP and PLANCK ( $\sigma_{\text{pix}}^2$  is the noise variance per pixel, and  $\Omega_{\text{pix}}$  the pixel solid angle). The correlation function is then given by the standard Legendre Polynomial expansion:

$$\langle \tau(\theta_1)\tau(\theta_2) \rangle = \frac{1}{2\pi} \sum_l \tilde{C}_l \left( l + \frac{1}{2} \right) P_l(\cos(\alpha)), \quad (28)$$

where  $\alpha$  is the angle between  $\theta_1$  and  $\theta_2$ .

<sup>3</sup>For example for a 900deg<sup>2</sup> survey there are  $N \simeq 9.10^7$  objects with  $I < 24$  mag.

The convergence correlation function is calculated as in Section 3, using the perturbation theory with the non-linear power spectrum evolution as described in Peacock & Dodds 1996.

#### 4.4. Results

We then performed a numerical integration of (26) for standard-CMD, open-CDM and  $\Lambda$ -CDM cosmological models. The signal-to-noise is given in the Table 1 for different cosmologies, smoothing lengths. The survey size is assumed to be  $900 \text{ deg}^2$ . The signal to noise ratio scales roughly like the square root of the area for larger surveys. A very good signal-to-noise ratio ( $\sim 9$ ) can be obtained at small smoothing scale, however even in the large smoothing scale case a significant detection can be obtained. This result contrasts with previous analysis of lensing on CMB where these typical signal-to-noise ratios were obtained with a whole sky survey.

Figure 3 shows how the signal-to-noise evolves with  $\theta_0$  for different values of the beam size  $\theta_0^{\text{CMB}}$ . The maximum signal-to-noise is obtained for  $\theta_0$  comparable to  $\theta_0^{\text{CMB}}$ , which is a consequence that at small scales the sheared galaxies behave essentially like a noise for the lensed temperature fluctuations, and at large scale the signal is smoothed away.

### 5. EFFECTS OF SECONDARY ANISOTROPIES

Undoubtedly, secondary anisotropies and foregrounds can affect our conclusions and should be examined in details. They may affect our calculations in three different ways: first some CMB fluctuations might be generated at low redshift and the assumption the source plane is located at  $z_{\text{source}} \simeq 1000$  breaks down; secondary anisotropies are correlated with low redshift mass concentrations which might introduce spurious correlations between CMB ellipticities and galaxy shear; galactic foregrounds can change our estimation of the cosmic variance. We compare in the next paragraphs the importance of various secondary effects.

#### 5.1. Thermal Sunyaev-Zeldovich (TSZ)

TSZ effect is the most important source of secondary anisotropies. It corresponds to the scattering of CMB photons on electrons of the hot cluster gaz. During the scattering, the photon energy is redistributed from the low frequency to high frequency part of the black body energy distribution. The net effect is a deficit of photons at low frequency (resp. an excess at high frequency), which creates a negative (resp. positive) fluctuation in the CMB map. Such fluctuations, essentially centered on clusters of galaxies (where the gaz is hot enough) creates a specific ellipticity pattern, correlated with the gravitational shear generated by those clusters. Therefore the ensemble average  $\langle \cos(\theta_g) \rangle$  (Eq.(17)) is not expected to vanish, even in the absence of gravitational lensing. The importance of this contribution depends on the amplitude and the extension of TSZ, and it is beyond the scope of this paper to perform an exact calculation. However we know that the amplitude of TSZ is proportional to the gaz temperature, which is important in the inner part of galaxy clusters only, at scales 1-2' (see Perci et al. 1995, where the TSZ is calculated). TSZ coming from larger scales

(filaments for instance) do not have a significant contribution (Tegmark et al. 1999). Therefore by observing the CMB at a resolution of 5' or larger, TSZ should not be a problem. For smaller scales it can become difficult to disentangle between the lensing effect and the ellipticity-shear correlation generated by TSZ. However we should emphasize that it is always possible to suppress this effect by either observing at 217 GHz (for which TSZ vanishes) or by cleaning TSZ taking advantage of its specific spectral signature.

#### 5.2. Kinetic Sunyaev-Zeldovich (KSZ) and Ostriker & Vishniac (OV) effects

Although these effects are sometime discussed separately in the literature, they have the same physical origin: this is a Doppler effect caused by the electron bulk motion. OV is a perturbative effect, while KSZ is a non-linear effect which can be important in the inner part of the clusters. OV is negligible at scale larger than 3', but its contribution increases quickly with decreasing scale, and equals the primary spectrum at 2' (Hu & White 1999). KSZ provides a significant increase of the OV only for scales smaller than 2' (Hu 1999). Therefore as long as we work at scales larger than 2-3', KSZ and OV are not important for our purpose. At smaller scales it become essential to estimate their contribution to  $\langle \cos(\theta_g) \rangle$ .

#### 5.3. Integrated Sachs-Wolfe (ISW) and Rees-Sciama effects (RS)

ISW and RS effects describe the frequency shift of a CMB photon when it crosses a time evolving gravitational potential well. The induced fluctuations are pure gravitational effects. The first order ISW occurs only for Universes different than ( $\Omega = 1, \Lambda = 0$ ) because for the flat  $\Omega = 1$  Universe the growth rate of structures is compensated by the Universe expansion. However there is always a non-linear ISW due to the time evolving potential of non-linear collapsing structures, which occurs in all cosmologies (the Rees-Sciama effect). The amplitude of RS was computed by Seljak 1996 who found a very small contribution for  $l < 4000$ . It is therefore irrelevant for our purpose.

#### 5.4. Galactic foregrounds and point sources

Tegmark et al. 1999 calculated the power spectrum contribution of galactic foreground and extra-galactic point sources. The galactic foreground contamination is dominant only at very large scales ( $l < 10$ ), but the point sources spectrum might become important for  $l > 1000$ . Fortunately the clustering properties of the point sources does not play a significant role (Toffolatti et al. 1998), therefore their contribution is essentially white noise, which makes their removal possible, as long as we have a good model for them (Guiderdoni 1999).

### 6. CONCLUSION

We have computed the amplitude of the correlation between the lensed CMB ellipticities and the lensed galaxy ellipticities to the leading order of perturbation theory. We found that the modulation of the relative angle distribution can be as high as 10% for a smoothing scale of 2.5' and 5% for 10'. This lensing effect extends to scales

well beyond the anisotropies generated by the foreground contamination and therefore it should be easily detectable with a low resolution experiment provided that the survey is large enough. In particular, future wide galaxy surveys (SLOAN) used jointly with all sky CMB experiments (MAP, PLANCK) are very promising for the measurement of such a lens effect. A sky coverage of only 30% will improve the signal-to-noise by a factor of 4 those given in Table 1. At scales larger than a few arcmin, any detected correlation between the CMB ellipticities and the shear of the distant galaxies can only be produced by lensing (since foregrounds contribution is too weak), this does not depend whether the CMB is intrinsically Gaussian or not (although we used the Gaussian approximation for the calculations).

At the arcmin scale and below, the secondary fluctuations becomes important, and the contribution of each foreground should be carefully estimated. Moreover, at such small scales, the CMB and shear fields cannot be ap-

proximated by Gaussian field, and one might go beyond by considering a weakly non-Gaussian distribution like the Edgeworth expansion.

The computation of the signal to noise ratio were made in a simplified way. In particular we assumed that the smoothing  $\theta_0^{\text{CMB}}$  for  $\kappa$  takes most of the effects associated with the beam smoothing, which we believe should be a good approximation as long as the ellipticity orientations only are concerned. We plan to check this aspect in numerical simulations.

We thank Simon Prunet and Dmitry Pogosyan for useful discussions on this subject and for a careful reading of the manuscript. We all thank IAP for hospitality and the Terapix data center (<http://terapix.iap.fr/>) for computing facilities. F.B. and K.B. thank CITA for hospitality. We thank M. Zaldarriaga and U. Seljak for the use of their code CMBFAST.

#### REFERENCES

- Benabed, K., and Bernardeau, F., astro-ph/9906161  
 Bernardeau, F. 1997, A&A, 324, 15  
 Bernardeau, F. 1998, A&A, 338, 767  
 Bond, J.R., and Efstathiou, G, 1987, MNRAS, 266, 655  
 Metcalf, R. B.; Silk, J., 1998, ApJ, 492, L1  
 Goldberg, D., and Spergel, 1998, astro-ph/9811251  
 Guiderdoni, B., 1999, astro-ph/9903112  
 Hu, W., 1999, astro-ph/9907103  
 Hu, W., and White, M., 1996, A&A, 315, 33  
 Peacock, J.A, and Dodds, S.J., 1996, MNRAS, 280, L19  
 Perci, F.M., Spergel, D., Cen, R., Ostriker, J., 1995, ApJ, 442, 1  
 Schneider, P., and Seitz, C., 1995, A&A, 294, 411  
 Seljak, U., 1996, ApJ, 460, 459  
 Seljak, U., and Zaldarriaga, M., 1996, ApJ, 469, 437  
 Seljak, U., and Zaldarriaga, M., astro-ph/9907254  
 Spergel, D., and Goldberg, D., 1998, astro-ph/9811252  
 Suginozono, M., Suginozono, T., Spergel, D. N., 1998, ApJ, 495, 511  
 Tegmark, M. et al., 1999, astro-ph/9905257  
 Toffolatti, M. et al., 1998, MNRAS, 297, 117  
 Zaldarriaga, M., and Seljak, U., Phys. Rev. D58 (1998) 023003  
 Zaldarriaga, M., and Seljak, U., Phys. Rev. D59 (1999) 123507

TABLE 1  
 VALUES OF  $\langle \cos(\theta_g) \rangle$  AND ITS SIGNAL-TO-NOISE

| Model                         | $\langle \cos(\theta_g) \rangle$ for $\theta_0 = 5'$ | $S/N$ for $\theta_0 = 2.5'$ | $S/N$ for $\theta_0 = 5'$ | $S/N$ for $\theta_0 = 10'$ |
|-------------------------------|--|-----------------------------|---------------------------|----------------------------|
| standard-CDM (900 $deg^2$ )   | 0.057  | 8.3                         | 5.4                       | 3.3                        |
| $\Lambda$ -CDM (900 $deg^2$ ) | 0.054  | 10.7                        | 6.7                       | 3.9                        |
| Open-CDM (900 $deg^2$ )       | 0.040  | 7.5                         | 4.4                       | 2.3                        |

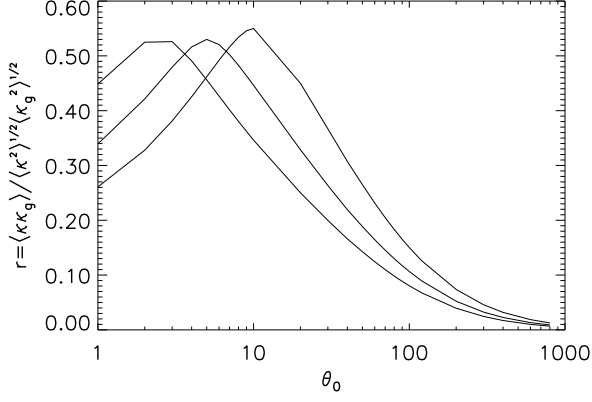


FIG. 1.— Correlation coefficient  $r = \langle \kappa \kappa_g \rangle / (\sigma \sigma_g)$  as defined in (15) for LCDM model for a galaxy source plane at  $z = 1$ .  $r$  is given as a function of the smoothing angle  $\theta_0$  for  $\kappa_g$ . The three curves from left to right correspond to a fixed beam size  $\theta_0^{\text{CMB}}$  of 2.5', 5' and 10'. The stronger correlation is obtained when  $\theta_0$  is comparable to the CMB beam size.

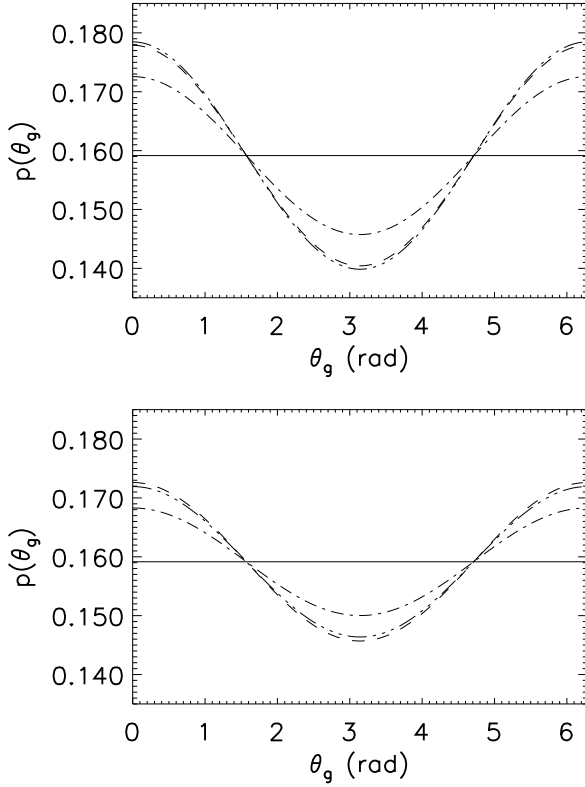


FIG. 2.— Probability distribution function of the relative orientation  $\theta_g$  between the CMB ellipticity and the sheared distant galaxies (Eq.16). The beam size is  $\theta_0^{\text{CMB}} = 2.5'$  for the upper plot and  $\theta_0^{\text{CMB}} = 10'$  for the lower plot, and the smoothing length of the convergence  $\kappa_g$  is respectively  $\theta_0 = 2'$  and  $\theta_0 = 10'$ . The horizontal solid line represents the uniform distribution of  $\theta_g$  in the un-lensed case. The dot-dashed line is for  $\Omega_M = 0.3$ ,  $\Lambda = 0$ ,  $\sigma_8 = 1$ , the triple dot-dashed line for  $\Omega_M = 0.3$ ,  $\Lambda = 0.7$ ,  $\sigma_8 = 1$  and the dashed line for  $\Omega_M = 1$ ,  $\Lambda = 0$ ,  $\sigma_8 = 0.6$ .

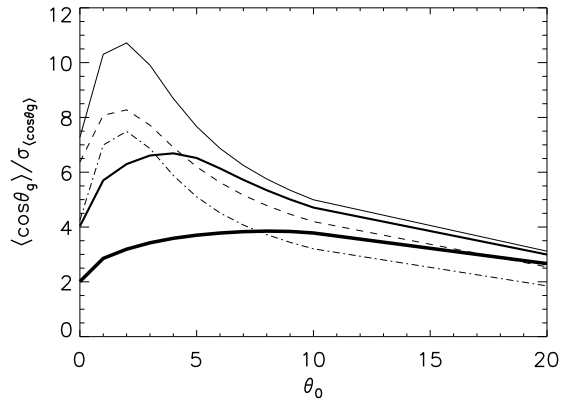


FIG. 3.— Signal-to-noise ratio of  $\langle \cos(\theta_g) \rangle$  as a function of the convergence smoothing scale  $\theta_0$ . The CMB and the galaxy surveys have both a size of  $900 \text{ deg}^2$ . The cosmological models are standard-CDM (dashed line), open-CDM (dotted line) and  $\Lambda$ -CDM (solid lines). The beam size is always  $2.5'$  except for the thick line ( $\Lambda$ -CDM, beam= $5'$ ) and thick thick line ( $\Lambda$ -CDM, beam= $10'$ ).